Desalination and Water Treatment
www.deswater.com

doi: 10.5004/dwt.2020.25216

182 (2020) 385–394
April

Decoloration of textile Acid Red 18 dye by hybrid UV/COP advanced oxidation process using ZnO as a catalyst immobilized on a stone surface

Mohammad Malakootian[a,b], Alfred Smith Jr.[c], Majid Amiri Gharaghani[d], Hakimeh Mahdizadeh[b,e,§], Alireza Nasiri[a], Ghazal Yazdanpanah[e,*]

[a]*Environmental Health Engineering Research Center, Kerman University of Medical Sciences, Kerman, Iran, emails: m.malakootian@yahoo.com (M. Malakootian), nasiri_a62@yahoo.com (A. Nasiri)*

[b]*Department of Environmental Health, School of Public Health, Kerman University of Medical Sciences, Kerman, Iran* [c]*Department of Biology, Foothill–De Anza Community College District, Los Altos Hills, CA, USA, email: bonk@att.net (A. Smith Jr.)*

[d]*Department of Environmental Health Engineering, Sirjan School of Medical Sciences, Sirjan, Iran, email: amiri.majid76@gmail.com (M. Amiri)*

[e]*Student Research Committee, Kerman University of Medical Sciences, Kerman, Iran, Tel. +98 343 132 5128, Fax: +98 343 132 5105; emails: ghazal.yazdanpanad@gmail.com (G. Yazdanpanah), H.Mahdizadeh2018@gmail.com (H. Mahdizadeh)*

Received 27 April 2019; Accepted 22 November 2019

ABSTRACT

Azo dyes are one of the most important groups of synthetic dyes. These dyes are compounds resistant against decomposition by biological processes and are used in textile industries. The aim of this study was to decoloration of textile Acid Red 18 dye by hybrid UV/catalytic ozonation process (COP) advanced oxidation process (AOP) using ZnO (synthesized by thermal method) as a catalyst, immobilized on a stone surface. The process efficiency was investigated using parameters of pH, contact time, catalyst concentration and initial concentration of dye in the hybrid process. Dye removal mechanisms were identified in the sole ozonation process, COP and photocatalytic process (UV/ZnO). X-ray diffraction, scanning electron microscopy and transmission electron microscopy analyses were used to study the structural properties, morphology, and size of the ZnO nanoparticles. 97% dye removal was obtained at a contact time of 40 min, pH: 5, catalyst concentration of 3 g/L and dye initial concentration of 25 mg/L. The Yazdbaf textile factory wastewater was selected as a real sample and its physicochemical quality was determined. Also, the Acid Red 18 dye removal efficiency was obtained 65% in the optimal conditions. Kinetic studies showed that the decomposition reaction follows pseudo-first-order kinetics. The UV/COP hybrid process as an AOP has high efficiency in removing resistant dye contaminants from textile wastewater.

Keywords: Azo dyes; ZnO; Wastewater; Textile industry; COP process

1. Introduction

Colored wastewater is the most important problem in the textile industry. Most dyes are compounds with complex structures and have characterizations such as toxicity, carcinogenicity, mutagenic effect, stability in the environment and low biodegradability [1,2]. In accordance with the color index (CI), more than 10,000 different dye types are synthesized and available in the world. Azo and anthraquinone dyes at 70% and 15% abundance in the textile industry respectively are the biggest groups in color categories. Approximately 700,000 tons of dyes are produced for various industrial applications around the world annually, of which about 50% is discharged into the environment

---

* Corresponding author.

§ Co-corresponding author.

through wastewater [3]. The variation in textile wastewater content from this high production has created problems in textile wastewater treatment. The discharge of textile wastewater into the environment and aquatic ecosystems leads to a decrease in water quality [4], prevention of penetration of light into deep water, disruption of the photosynthesis process, interference in the ecology of receiving waters, and the loss of plant life. Also, these compounds are toxic, carcinogenic and mutagenic, effects causing irreparable damage to the environment; therefore, effective and efficient treatment of these compounds is a necessity for the preservation of the environment [5]. The complex aromatic structure of dyes makes them more stable and difficult to remove from wastewater discharged into receiving waters. As well as, in Iran, many carpet weaving, cloth printing, and textile industries produce many non-separable dyes, which cause environmental complications [6]. Azo dyes are one of the most important groups of artificial colors that because of low price, high solubility and stability are used in textile industries. These compounds are resistant to biodegradation and do not decompose under aerobic conditions. Some processes used for dye color removal in the textile industry are biological purification [7,8], bioelectrochemical system integrated with a membrane biofilm reactor [7], pyrolysis technique [9], Fenton and Fenton-like [10], ion exchange [11], adsorption [12,13], photocatalyst [14,15], electrolysis [16–18], and membrane processes [19]. Each of these methods has advantages and disadvantages. Removal of resistant pollutants such as dyes in biological systems occurs slowly and under certain biological conditions [3,5]. Some methods such as surface absorption, ion exchange, and membrane processes cannot decompose pollutants and only cause the transfer of pollutants from one phase to another, creating secondary pollution needing to be refined again. In addition, some limitations of these methods are membrane blocking, adsorbent surface saturation and the need to wash and regenerate the adsorbents and resins, which increases the costs. Therefore, the application of most of these techniques is not pervasive in industries. Advanced oxidation processing (AOP), as a green technology based on situ generations that produce strong destructive radicals such as hydroxyls ($OH^\bullet$), does not have the aforementioned limitations [20]. Hydroxyl radicals with high oxidizing ability react with color molecules, destroying them and converting them into harmless organic compounds such as CO_2 and H_2O·UV/H_2O_2, O_3, Fenton, ultrasonic and photocatalytic degradation, etc. are the most widely used AOPs [21]. The application of ozonation for decolorization and removal of organic materials is often under consideration by many researchers as a viable AOP process [22]. Negatively, ozone application for direct removal of pollutants has limitations such as high energy consumption for ozone production, incomplete degradation of some resistant compounds and ozone selectivity. Yet positively, in some cases the application of catalysts in the catalytic ozonation process (COP) can cause an increase in the production of destructive radicals, leading to increased ozonation process efficiency and subsequent process cost reduction [22]. Metal ferrites and metal oxides like $CoFe_2O_4$, $ZnFe_2O_4$, Fe_2O_3, MnO_2, Ce_2O_3, WO_3, TiO_2, ZnO, CoO, Al_2O_3, and MgO, etc. are solid catalysts that are widely used in the photocatalytic processes [23–30]. Among the various metal catalysts, a ZnO catalyst was chosen for study because of low cost, wider band and better stimulation by ultraviolet irradiation [31]. If the COP process is exposed to UV radiation, the process of photo-catalysis occurs simultaneously [32]. The UV/COP process as a new hybrid oxidation advanced process has properties such as prevention of secondary pollution in the environment, strong degradation ability, reduced need of increasing the oxidizing agent's dose, high process speed and suitability for organic pollutants removal. In the hybrid AOP UV/COP organic materials in wastewater are removed through several types of mechanisms simultaneously (Fig. 1) [32].

Oxidation of organic compounds and indirect oxidation by H_2O and OH radicals which are produced as a result of ozone degradation in the water can cause contaminants' destruction [33]. Ozonation process efficiency increases with the addition of UV rays (O_3/UV) and a metal catalyst [34]. The organic oxidation mechanism in O_3/UV and COP processes is based on hydroxyl radical production and resulting

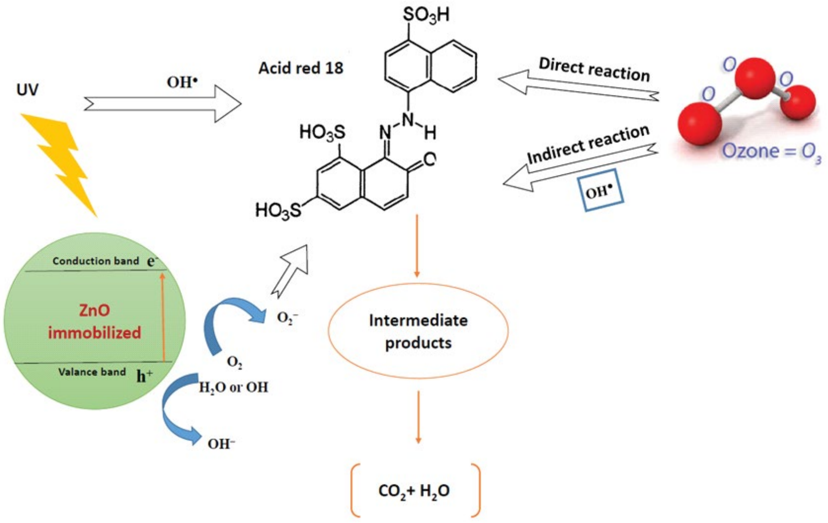

Fig. 1. Acid Red 18 dye removal mechanisms in the hybrid advanced oxidation process UV/COP.

in effective contaminant degradation [34]. In addition, the photocatalytic degradation process also occurs simultaneously. In photocatalytic degradation, energy comes from UV rays or sunlight shining as photons on ZnO immobilized on a stone surface, and this causes electron excitation in the valence bands of ZnO, with the electron moving to the conduction band. This electron transformation makes a hole (h^+) in the valence band. H^+ reacts with water and hydroxide and a hydroxyl-reactive radical is produced [31,35].

In this process recycling and light scattering in suspension and the electrons and holes recombination in catalysts are the problems that can be pointed out which could reduce consequently, degradation efficiency and hydroxyl production. To solve these problems some methods such as nanoparticles immobilization on a media and the use of strong oxidants like ozone along with a photocatalytic process are recommended [18]. Immobilizing nanoparticles on inert surfaces enable their reuse, and the significant reduction in the number of nanoparticles in outlet wastewater makes nanoparticle removal methods such as filtering and centrifuging outlet wastewater unnecessary [36,37]. Ozone is a powerful oxidant that has high oxidation potential (2.07) and shows high efficiency when it combines with other processes. Ozone has a lot of advantages such as a reduction in toxic byproducts production, short reaction time, etc. The aim of this study is the decoloration of textile Acid Red 18 dye by hybrid UV/COP AOP using ZnO as a catalyst immobilized on a stone surface, and determining the effective parameters in the removal process, with the recommendation of new methods in environmental wastewater management in these industries.

2. Materials and methods

CH_3CH_2OH, H_2SO_4, NaOH, $ZnSO_4$, $7H_2O$ and Na_2CO_3, all 99.8% pure, were provided by Merck & Co. (Germany). Acid Red 18 dye at 99.9% purity was obtained from Alvan Paint Company (Tehran, Iran). Flat, rough waste stones of suitable dimension for the reactor floor-standing were used as a catalyst bed.

2.1. Synthesis of ZnO nanoparticles by thermal method

ZnO nanoparticles were synthesized by a thermal method based on $Zn_4(SO_4)(OH)_6\cdot 0.5H_2O$ conversion. First, a 0.5 molar solution of $ZnSO_4\cdot 7H_2O$ and a 0.4 molar solution of Na_2CO_3 were prepared. Next, sodium carbonate solution was added drop by drop to zinc sulfate solution to form $Zn_4(SO_4)(OH)_6\cdot 0.5$ in H_2O at 70°C for 45 min with high-speed mixing [38]. The sediment was collected by the filter. Sediment was washed several times with distilled water and ethanol then dried at 70°C in the oven. The obtained precursor was immobilized on 3 pieces of flat and rough stone 3 in 20 cm and to calcination it was placed in an electric furnace (BADi) for 1 h at 850°C.

2.2. Reactor design and operation

All experiments were done in a laboratory-scale reactor. A plexiglass reactor was used in testing, with dimensions of 10 cm × 25 cm × 5 cm, made as shown in Fig. 2. Three UV-C lamps (6-watt) were placed on the reactor. Ozone generators (Modular Ozone Generator, France) were used to produce ozone, which was injected into the reactor by air bubbles at a fixed rate of 4 L/min (3 mg/min). The distance between the catalyst bed surface and the UV irradiation source, used together to produce hydroxyl radicals, was set at approximately 2 cm. To mix materials in the reactor a peristaltic pump with a flow rate of 1 mL/s was used.

A synthetic solution of Acid Red 18 with a specific concentration (1,000 mg/L) was prepared and stored in a dark place. The initial pH of the solution was adjusted using HNO_3 and H_2SO_4 and was measured by a pH meter (HANNA model, Japan). To investigate the effects of various concentrations of color (25, 50, 75, and 100 mg/L), different pH's (4, 7, 9, and 11), and different times in removal of color rate (5, 10, 15, 20, 25, 30, 35, and 40 min), 350 ml of solution with specific varying concentrations and pH was poured inside the reactor in the presence of the UV lamp and ozone. The effects of various processes such as photolysis, COP, sole ozonation process (SOP) and photocatalysis were evaluated. The physicochemical quality of

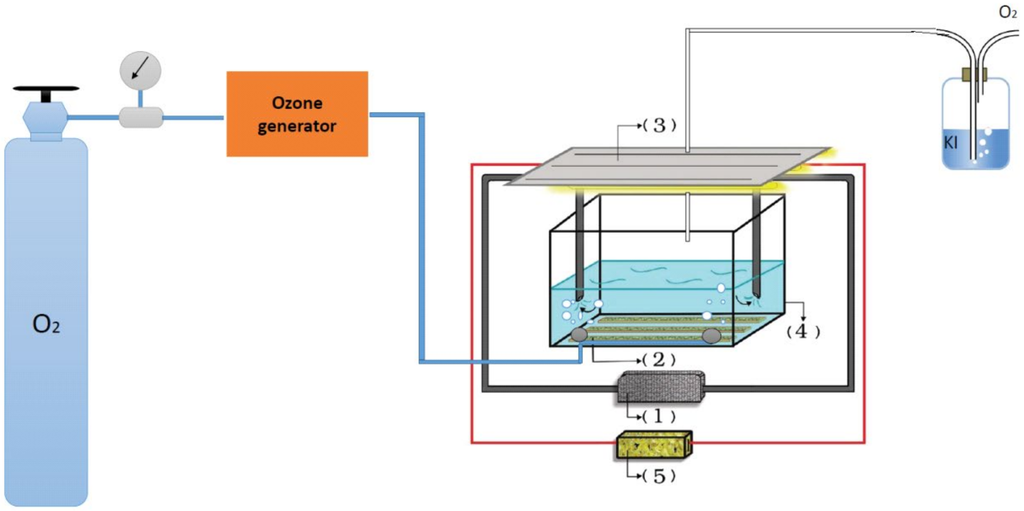

Fig. 2. Peristaltic pump (1), ZnO synthesized nanoparticles on stone bed (2), UV lamp (3), cubic reactor (4), and Transformer (5).

Yazdbaft textile factory wastewater (Yazd, Iran) was determined and the amount of dye removal was evaluated in the optimum conditions. Due to the low concentration of Acid Red 18 in wastewater, this dye was added to the wastewater sample until the dye concentration reaches to 25 mg/L.

Initial concentration and color output at a wavelength of 507 nm was measured by using a UV spectrophotometer (Shimadzu model, Japan). An X-ray diffraction analyzer (XRD) (Philips X'PERT, Netherlands) was used to determine the constituent phases and the crystalline size of ZnO nanoparticles immobilized on the stone surface. To determine the morphology, microscopic structure, and synthesized ZnO nanoparticles' size, a scanning electron microscopy (SEM) (KYKY-EM3200, China) and transmission electron microscopy (TEM: Philips CM30, Netherland) were used. The reaction kinetics were studied with the pseudo-first-order equation. The results were analyzed by using SPSS-22 software.

3. Results and discussion

3.1. Characterization of ZnO catalyst

XRD analysis was used to evaluate the phase structure changes and the crystalline size of ZnO nanoparticles immobilized on the stone. The XRD pattern of the ZnO nanoparticles synthesized by thermal method and calcined at 850°C is shown in Fig. 3.

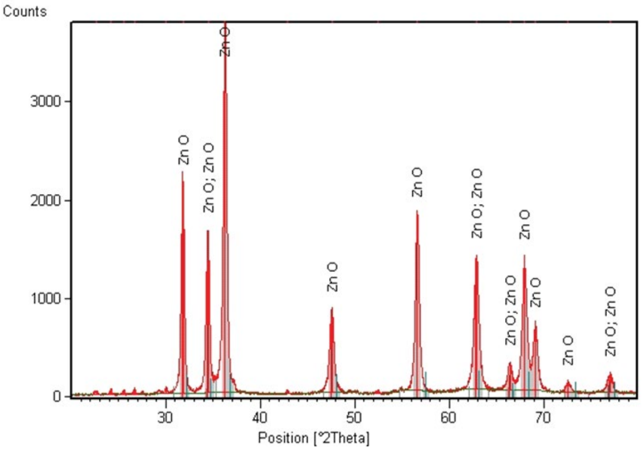

Fig. 3. XRD diffraction of ZnO nanoparticles.

The presence of 31.8°, 34.5°, 36.3°, 47.5°, 56.5°, 62.8°, 66.2°, 68°, 69°, 72.5°, and 77° in XRD pattern is in accordance with hexagonal wurtzite structure of ZnO nanoparticles which is in agreement with JCPDS standard cards no. 05-0664. It shows that the ZnO crystalline structure did not change at high temperatures. No extra peaks were observed in this diffraction, which indicates the synthesis of pure ZnO nanoparticles. In addition, the peaks' severity and their narrow width are indicative of high purity crystalline nanoparticles [39,40].

Fig. 4 shows SEM images of the ZnO nanoparticles' morphology and size, after being synthesized under thermal conditions.

In the investigation of the SEM results, ZnO nanoparticles ranging in size from 40.4 to 89.3 nm were observed in spherical and semi-spherical structures. In addition, the nanoparticle surfaces are rough and porous. The images obtained from TEM analysis were investigated to achieve more information about hollow spherical and semi-spherical ZnO structures [40]. Fig. 5 shows TEM images of the ZnO semi-spherical structures, which confirm their hollow structures.

3.2. Mechanism and effect of involved processes in dye removal by the hybrid process UV/COP

Using the hybrid AOP UV/COP, the amount of Acid Red 18 dye removal was tested simultaneously under the influence of several types of degradation processes such as photolysis (UV), SOP, COP and photocatalysis (ZnO/UV). To determine the effect of each process, the dye removal efficiency for each process was evaluated separately in the same conditions and the results are compared in Fig. 6.

As shown in Fig. 6, with Acid Red 18 dye at an initial concentration of 25 mg/L, neutral pH (6.5), and after contact time 40 min in photolysis (UV), photocatalysis (ZnO/UV), SOP, ozonation under UV irradiation and UV/COP ozonation processes, a removal rate was obtained at 36%, 86.5%, 86%, 90%, and 97%, respectively. The minimum dye removal is related to the photolysis (UV) process. It is clear that due to the dye's high stability and complex structure the molecule

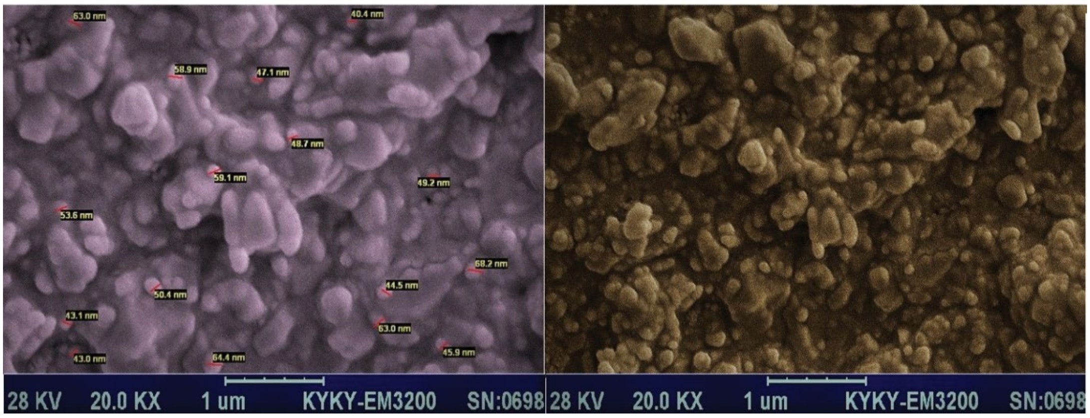

Fig. 4. SEM images of ZnO nanoparticles synthesized by using thermal method, immobilized on a stone surface.

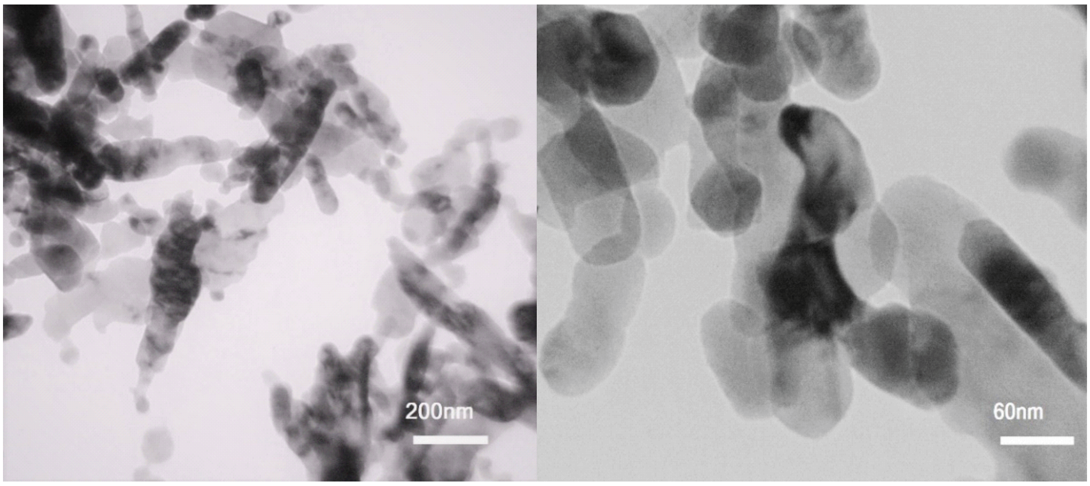

Fig. 5. TEM images of synthesized ZnO nanoparticles by using thermal method, immobilized on a stone surface.

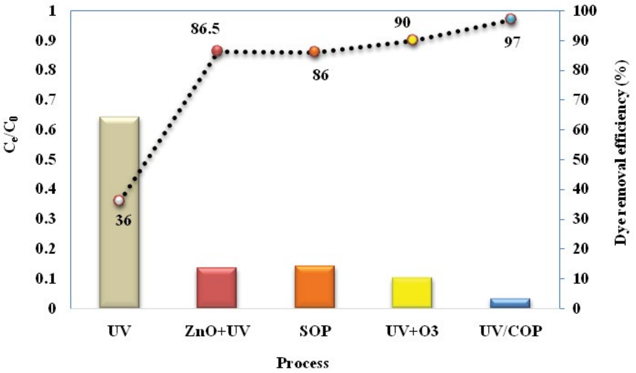

Fig. 6. Effect of involved processes in the Acid Red Dye 18 removal rate with a hybrid UV/COP process (dye initial concentration: 25 mg/L, contact time: 40 min, and pH: 6.5).

breakdown by direct photolysis is not easily possible and takes a lot of time [41]. In the SOP process, ozone degrades dye molecules by two mechanisms: 1. Ozone directly attacks a specific part of the dye molecule and degrades it. 2. Ozone molecules degrade and produce hydroxyl radicals. These radicals have high destructive property. Both types of mechanisms are important but ozone molecules contribute less than hydroxyl radicals toward this pollutant's resistance to degradation [5,36]. Also, because of high energy consumption, the application of ozone alone is not affordable for the complete degradation of resistant organic materials. The ozone process efficiency increases in combination with other factors such as UV, catalyst, etc. (Eqs. (1)–(4)) [5,34,36,42,43].

$$O_3 + H_2O + hv \rightarrow O_2 + H_2O_2 \tag{1}$$

$$H_2O_2 + hv \rightarrow 2{}^\bullet OH \tag{2}$$

$$O_3 + H_2O_2 \rightarrow HO_2^{-\bullet} + HO^\bullet + O_2 \quad K = 1.0 \times 10^{-2}\,M^{-1}S^{-1} \tag{3}$$

$$H_2O_2 \leftrightarrow HO_2^- + H^+ \tag{4}$$

According to Eqs. (5)–(12) in the photocatalytic process of (ZnO/UV) UV irradiation on the ZnO immobilized on a stone surface, the ZnO undergoes optical excitation and ZnO valence band electrons move to the conduction band. These excited electrons transferred to the conduction band leave positive holes in the ZnO catalyst valence band, which facilitates destructive hydroxyl radical formation [6,35].

$$ZnO + hv \rightarrow ZnO\left(e_{CB}^- + h_{VB}^+\right) \tag{5}$$

$$h_{VB}^+ + H_2O \rightarrow {}^\bullet OH + H^+ \tag{6}$$

$$h_{VB}^+ + OH^- \rightarrow {}^\bullet OH \tag{7}$$

$$h_{VB}^+ + \text{Acid Red } 18^{\bullet +} \rightarrow \text{Oxidation Acid Red } 18 \tag{8}$$

$$e_{CB}^- + O_2 \rightarrow {}^\bullet O_2^- \tag{9}$$

$${}^\bullet O_2^- + HO_2^\bullet + H^+ \rightarrow H_2O_2 + O_2 \tag{10}$$

$${}^\bullet O_2^- + \text{Acid Red } 18 \rightarrow \text{Acid Red } 18^{\bullet +} \rightarrow \text{Oxidation Acid Red } 18 \tag{11}$$

$$OH^\bullet + \text{Acid Red } 18 \rightarrow \text{Acid Red } 18^{\bullet +} \rightarrow \text{Oxidation Acid Red } 18 \tag{12}$$

In the photocatalytic process, some limitations such as catalyst optical corrosion by UV irradiation inhibit environmental pollutant removal. Furthermore, free excited electrons can fill available catalyst valence band electron positions and reduce photocatalytic activity [37]. In this study the maximum dye removal observed was with the hybrid UV/COP process. According to Eqs. (13)–(18), with the UV/COP process both the hydroxyl radical production and dye removal efficiency were increased [6,32,37,43,44].

$$\mathrm{ZnO} + h\nu \rightarrow e^- + h^+ \qquad (13)$$

$$\mathrm{O_3} + e^- \rightarrow \mathrm{O_3^{\bullet-}} \qquad (14)$$

$$\mathrm{O_3^{\bullet-}} + \mathrm{H^+} \rightarrow \mathrm{O_2} + \mathrm{HO_3^{\bullet}} \qquad (15)$$

$$\mathrm{HO_3^{\bullet-}} \rightarrow \mathrm{O_2} + \mathrm{HO^{\bullet}} \qquad (16)$$

Therefore, the application of advanced oxidation integration systems overcomes some problems and limitations in each sub-process and increases the efficiency and stability of water and wastewater treatment systems. Hassani et al. [45] in their study entitled "Photocatalytic ozonation of ciprofloxacin from aqueous solution using TiO_2/MMT nanocomposite: nonlinear modeling and optimization of the process via artificial neural network-integrated genetic algorithm" concluded that ciprofloxacin at a concentration of 20 mg/L with the presence of nanoparticles at concentration 0.04 g/L, pH: 5 and subject to 30 min of photocatalytic ozonation processing had a 90% removal rate, which is higher than the ozonation, photolysis, adsorption, catalytic ozonation, and photocatalytic processes removal rates. These results are consistent with the results of this study.

3.3. Effect of Acid Red 18 initial concentrations

The effect of Acid Red 18 initial concentrations in the range of 25–100 mg/L under optimal conditions was investigated. The results are shown in Fig. 7.

By increasing the color concentration from 25 to 100 mg/L, the removal efficiency decreased from 97% to 69%, at a contact time of 40 min. The dye initial concentration is an important parameter in the degradation rate and the removal rate correlates with the dye initial concentration. In the AOP, hydroxyl radicals are produced but the number of these radicals is limited. So obviously, under the same conditions, the number of produced radicals will be the same and by increasing the dye concentration, the number of produced radicals will not be sufficient for all dye molecules to completely degrade. For full molecule degradation, more contact time is required, and a higher number of radicals is needed to react [20,46,47]. Mahmoodi et al. [46] study in 2011 investigated color degradation by copper ferrite nanoparticles in the photocatalytic ozonation process and observed that by increasing the color's initial concentration from 50 to 200 mg/L, the removal efficiency was reduced. The highest removal rate was at a concentration of 50 mg/L.

3.4. Effect of dose of ZnO as a catalyst immobilized on a stone surface

To investigate the effect of immobilized ZnO on dye removal efficiency in the UV/COP process, concentrations of 1, 2, and 3 g of synthesized nanoparticles were immobilized on stone surfaces and the dye removal rate was investigated at an initial dye concentration of 25 mg/L. The results are shown in Fig. 8.

By increasing the nanoparticle concentration from 1 to 3 g/L, the dye removal efficiency was increased from 86% to 97%. In the hybrid UV/COP process, ZnO nanoparticles play an important role. According to Eqs. (5)–(16), these nanoparticles as a catalyst have an effective role in photocatalytic degradation and the COP process. Increased ZnO concentration produces more photocatalyst active sites, and combined with UV increasing the electron excitation rate, more hydroxyl radicals are generated [31,47]. In a study conducted by Vaiano regarding advanced photocatalytic phenol removal using modified ZnO nanoparticles by silver, the ZnO/Ag photocatalytic activity was increased significantly by increasing nanoparticle concentrations from 0.075 to 0.15 g, and subsequently, the phenol removal efficiency also was increased. But no significant changes were observed at higher concentrations [48]. Khataee et al. [49] in a 2017 study in Iran demonstrated that by increasing the montmorillonite nanocomposite dose metronidazole removal efficiency increased. The reason for increased efficiency is the increased number of catalytic sites.

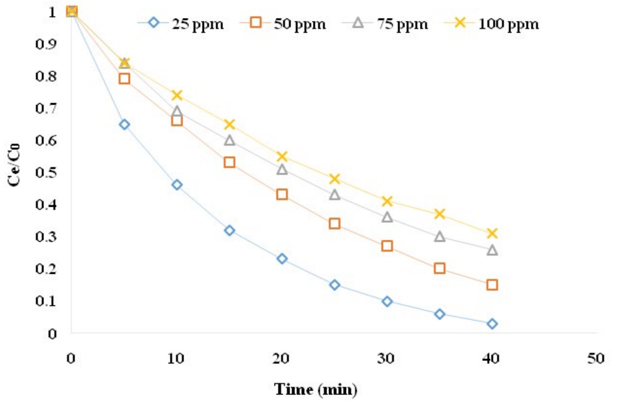

Fig. 7. Effect of dye initial concentration on the efficiency of the hybrid UV/COP process (contact time: 40 min, pH: 5, catalyst concentration 3 g/L, and O_3: 3 mg/min).

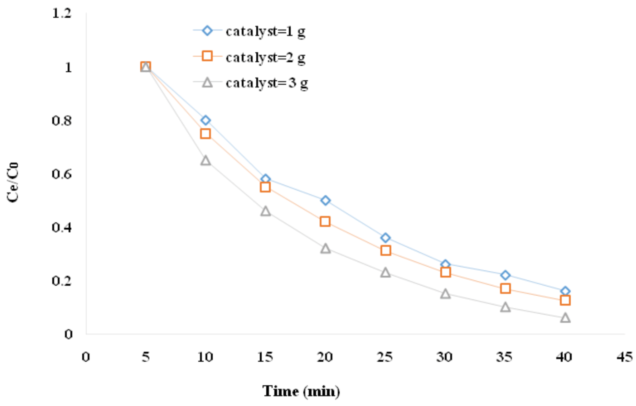

Fig. 8. Effect of catalyst concentration on the hybrid UV/COP process efficiency (contact time: 40 min, pH: 5, initial color concentration: 25 mg/L, and O_3: 3 mg/min).

3.5. Effect of pH

pH is one of the most effective parameters affecting AOPs. The effect of pH on Acid Red 18 dye degradation was investigated in the range of pH 3–11. The results are shown in Fig. 9.

In the hybrid UV/COP process, no significant fluctuations were observed in dye removal efficiency by changing the solution's initial pH. By increasing the solution initial pH from 4 to 7, the removal efficiency decreased from 97% to 90%. Further increasing the pH from 7 to 11 resulted in the removal efficiency increasing again from 90% to 92%. These fluctuations could be related to the SOP and photocatalytic processes efficiencies at different pH. In the SOP processes, changes in pH can cause significant changes in the process efficiency. According to Eqs. (17) and (18) in the SOP and UV/O_3 process, acidic and neutral pH have less contribution than basic pH in the removal of organic materials. In alkaline conditions, ozone molecules degrade, and destructive radicals such as $O_3^{\bullet-}$, $O_2^{\bullet-}$ and ${}^{\bullet}OH$ are produced [31,48,50]. The OH radical oxidation potential is 2.33 V while the ozone oxidation potential is 2.07 V. With hydroxyl radicals in alkaline conditions the process efficiency is increased compared with ozonation, as in alkaline conditions hydroxyl radicals degrade dyes rapidly and non-selectively [42,51].

$$O_3 + OH^- \rightarrow O_2 + HO_2^- \tag{17}$$

$$O_3 + HO_2 \rightarrow \text{Intermediate products}\left(O_3^{\bullet-}, O_2^{\bullet-}, {}^{\bullet}OH\right) \tag{18}$$

ZnO oxidizes to Zn^{2+} according to Eq. (19). It should be noted that the ZnO photocatalytic process efficiency in acidic conditions is higher than in alkaline conditions. The catalyst surface gets a positive charge and more dye molecules adsorb on the catalyst surface, which subsequently increases the removal efficiency [31,48].

$$ZnO + 2h_{VB}^{+} \rightarrow Zn^{2+} + O^{*} \tag{19}$$

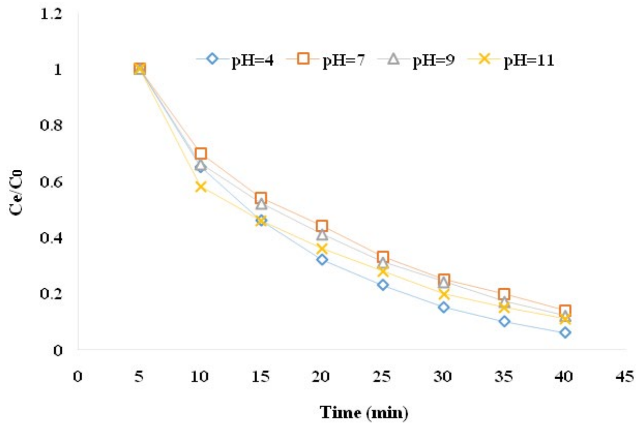

Fig. 9. Effect of the solution initial pH on the hybrid UV/COP process efficiency (contact time: 40 min, dye initial concentration: 25 mg/L, catalyst concentration: 3 g/L, and O_3: 3 mg/min).

The efficiency of the SOP and the photocatalytic processes decrease in acidic and basic conditions, respectively. Therefore, the application of the UV/COP hybrid system overcomes the other processes constraints and can be used for environmental pollutants removal from different types of wastewater with differing acidity.

Many researchers have observed that the organic compounds degradation in ozone hybrid oxidation processes is directly affected by the pH. In the Parsa et al. [52] study, the maximum Acid Red 18 degradation by ozone-electrolysis process was obtained at pH = 2. Because at low pH, the maximum dye molecules degradation occurs by direct reaction with ozone while hydroxyl radicals showed significant effect at high pH. It shows that ozone molecules effectively oxidize Acid Red 18 chromophore molecules compared to hydroxyl radicals, which leads to an increase in the degradation rate at low pH. Furthermore, the application of the ozonation hybrid with the electrolysis process at acidic pH was increased the process efficiency [52].

In another research, Parvarideh et al. [53] performed a comparative study on the malachite green dye decolorization by the catalytic ozonation and ozonation processes. The results showed that the malachite green dye decolorization rate in the alkaline condition was more effective than the acidic and neutral conditions in the ozonation process. But, in COP processes, there was no significant effect on the malachite green dye decolorization rate in the acidic, alkaline and neutral conditions [53]. These results conform to the present study.

3.6. Degradation kinetics

Pseudo-first-order kinetics are used to describe the dye removal. This model is commonly used for Azo dye degradation in AOPs and color removal in liquid leachate. Hence, the kinetic of Acid Red 18 degradation was evaluated at concentrations of 25, 50, 75, and 100 mg/L and in the range of 0–40 min using the first-order kinetic model according to Eq. (20) [6,31]. Then the required time to achieve the 99% removal efficiency was calculated from Eq. (21) [54].

$$\ln\left(\frac{C_0}{C_t}\right) = -K_1 t \tag{20}$$

$$t_{99} = \frac{-\ln 0.01}{k} \tag{21}$$

where K_1 is the first-order kinetic equation rate constant (1/min), C_0 is the equilibrium concentration and C_t is the concentration at time "t" [6]. Fig. 10 shows the pseudo-first-order kinetics diagram of dye degradation in the hybrid UV/COP process. By drawing Ln(C_0/C_t) in contrast to the reaction time the linear graph was obtained which calculated the rate constant with it.

In Table 1 the rate constant (k), the correlation coefficient (R^2), and the time required to degrade 99% of the Acid Red 18 dye are shown.

The results of Table 1 show that Acid Red 18 dye removal efficiency of 99% was obtained between 56 and 165 min in

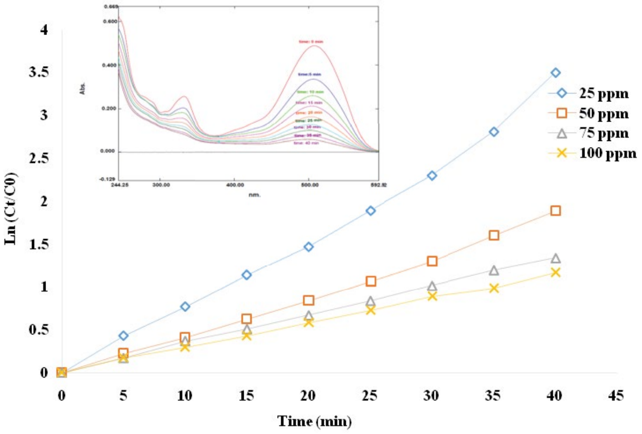

Fig. 10. Kinetics of Acid Red 18 degradation in the hybrid UV/COP process (pH: 5, catalyst concentration 3 g/L, and O_3: 3 mg/min).

the hybrid UV/COP process. The correlation coefficient (R^2) of more than 99% in the pseudo-first-order kinetics equation for different color concentrations confirms that the pseudo-first-order kinetics model is suitable for describing the Acid Red 18 dye degradation rate. Also, the rate constant speed decreases by increasing the color concentration [54,55]. Orge et al. [55] in their study entitled "Photocatalytic ozonation of aniline with TiO_2 carbon composite materials" achieved similar results. The most important mechanism in the AOP is the active hydroxyl radical production, with high oxidation potential; by combining oxidation processes more hydroxyl radicals are produced and the reaction speed increases.

3.7. Influence of interference pollutant on dye removal rate

The results of the Yazdbaf textile factory wastewater quality analysis and the dye removal efficiency in the optimum conditions are shown in Table 2.

The influence of interference pollutants in the real sample was investigated. As can be seen in Table 2, the dye removal efficiency decreased from 97% in the synthetic sample to 65% in the real sample. In the hybrid UV/COP AOP in the presence of ozone, the organic compounds degraded through two types of mechanisms. Ozone directly reacts with compounds that have double bonds and free radicals that generated from ozone, indirectly react with organic matters. The produced ozone and hydroxyl radicals, use to degrade the dye molecules and intermediates which produced from dye decomposition in synthetic sample [49,50]. In the real sample, ozone directly reacts with organic matters in the wastewater such as detergents and benzene. But the produced hydroxyl radicals from UV/O_3 non-selectively reacts with all compounds in the wastewater which leads to reduce the dye molecules removal efficiency.

Table 1
First-order kinetic rate constants and the time required to degrade 99% of the Acid Red 18 dye in the hybrid UV/COP process (pH: 5, catalyst concentration: 3 g/L, and O_3: 3 mg/min)

C_0 (mg/L)	R^2	K (1/min)	t_{99} (min)
25	0.9887	0.083	55.5
50	0.9947	0.046	100
75	0.9992	0.033	139.5
100	0.9987	0.028	164.5

Table 2
Results of the Yazdbaf textile factory wastewater quality analysis and the dye removal efficiency in the optimum conditions (contact time: 40 min, pH: 5, catalyst concentration: 3 g/L, O_3: 3 mg/min)

Analysis	Results
pH	8.9
Electrical conductivity (µs/cm)	4,850
Turbidity (NTU)	660
Chemical oxygen demand (mg/L)	3,200
Biochemical oxygen demand (BOD_5) (mg/L)	350
Total dissolved solids (mg/L)	9,000
Total suspended solids (mg/L)	2,800
Detergent (mg/L)	120
Benzene (mg/L)	145
Cr (mg/L)	18
Pb (mg/L)	30
Ni (mg/L)	14
Removal efficiency of Acid Red 18 (%)	65%

4. Conclusion

In this study, the UV/COP hybrid oxidation process was used for Acid Red 18 dye removal from textile wastewater. The color removal processes, mechanisms, including SOP, COP, and photocatalysis were investigated and the optimal removal conditions were identified in the hybrid process. A maximum dye removal rate using the UV/COP hybrid process was obtained at a contact time of 40 min and an initial concentration of 25 mg/L. The hybrid process has high efficiency in all pH ranges. pH change did not produce a significant change in the efficiency process. As shown, this process in both acidic and basic conditions has the ability to remove resistant organic compounds, overcomes some problems and limitations of added processes, and can be used for some environmental pollutants removal in different industries.

Acknowledgments

This research was conducted at the Environmental Health Engineering Research Center and was sponsored by the Vice-Chancellor for Research and Technology of Kerman University of Medical Sciences. A note of appreciation is expressed here to the Vice-Chancellor and to all university staff who provided assistance to make this study possible.

References

[1] G. Moussavi, M. Mahmoudi, Degradation and biodegradability improvement of the reactive red 198 azo dye using catalytic ozonation with MgO nanocrystals, Chem. Eng. J., 152 (2009) 1–7.

[2] S. Mozia, M. Tomaszewska, A.W. Morawski, A new photocatalytic membrane reactor (PMR) for removal of azo-dye Acid Red 18 from water, Appl. Catal., B, 59 (2005) 131–137.

[3] A.R. Rahmani, F.B. Askari, G. Asgari, M.T. Samadi, Degradation of reactive red 198 dye by catalytic ozonation using pumice and copper coated pumice, Fresenius Environ. Bull., 21 (2012) 2810–2817.

[4] M. Malakootian, Z. Darabi-Fard, N. Amirmahani, A. Nasiri, Evaluation of arsenic, copper, lead, cadmium, and iron concentration in drinking water resources of central and Southern Bardsir plain, Iran, in 2014, J. Kerman Univ. Med. Sci., 22 (2015) 542–554.

[5] F. Bahrami-asl, M. Kermani, S. Salahshour-Arian, M. Mollamahmoudi-Abadi, D. Zeynalzadeh, Catalytic ozonation of azo dye Reactive Red 120 in the presence of MgO nanoparticles, J. Health Field, 2 (2017).

[6] B. Krishnakumar, M. Swaminathan, Influence of operational parameters on photocatalytic degradation of a genotoxic azo dye Acid Violet 7 in aqueous ZnO suspensions, Spectrochim. Acta, Part A, 81 (2011) 739–744.

[7] Y. Pan, T. Zhu, Z. He, Enhanced removal of azo dye by a bioelectrochemical system integrated with a membrane biofilm reactor, Ind. Eng. Chem. Res., 57 (2018) 16433–16441.

[8] Y. Liu, K. Li, W. Xu, B. Du, Q. Wei, B. Liu, D. Wei, GO/PEDOT: NaPSS modified cathode as heterogeneous electro-Fenton pretreatment and subsequently aerobic granular sludge biological degradation for dye wastewater treatment, Sci. Total Environ., 700 (2020), https://doi.org/10.1016/J.SCITOTENV.2019.134536.

[9] M. Kafil, S.B. Nasab, H. Moazed, J. Jokiniemi, A. Lahde, A. Bhatnagar, Efficient removal of azo dyes from water with chitosan/carbon nanoflower as a novel nanocomposite synthesized by pyrolysis technique, Desal. Wat. Treat., 142 (2019) 308–320.

[10] N.C. Fernandes, L.B. Brito, G.G. Costa, S.F. Taveira, M.S.S. Cunha–Filho, G.A.R. Oliveira, R.N. Marreto, Removal of azo dye using Fenton and Fenton-like processes: evaluation of process factors by Box–Behnken design and ecotoxicity tests, Chem. Biol. Interact., 291 (2018) 47–54.

[11] S. Karcher, A. Kornmüller, M. Jekel, Anion exchange resins for removal of reactive dyes from textile wastewaters, Water Res., 36 (2002) 4717–4724.

[12] S.N. Jain, P.R. Gogate, Adsorptive removal of azo dye in a continuous column operation using biosorbent based on NaOH and surfactant activation of *Prunus dulcis* leaves, Desal. Wat. Treat., 141 (2019) 331–341.

[13] S.P. Santoso, A. Kurniawan, F.E. Soetaredjo, K.-C. Cheng, J.N. Putro, S. Ismadji, Y.-H. Ju, Eco-friendly cellulose–bentonite porous composite hydrogels for adsorptive removal of azo dye and soilless culture, Cellulose, 26 (2019) 3339–3358.

[14] R. Jiang, H.-Y. Zhu, S.-T. Jiang, Y.-Q. Fu, E.-M. Zong, J.-B. Li, G.-M. Zeng, Magnetically separable Fe_3O_4/BiOBr microspheres: synthesis, characterization, and photocatalytic performance for removal of anionic azo dye, Environ. Eng. Sci., 36 (2019) 466–477.

[15] L. Kőrösi, B. Bognár, S. Bouderias, A. Castelli, A. Scarpellini, L. Pasquale, M. Prato, Highly-efficient photocatalytic generation of superoxide radicals by phase-pure rutile TiO_2 nanoparticles for azo dye removal, Appl. Surf. Sci., 493 (2019) 719–728.

[16] A. Khosravi, Z.H. Rad, N. Amirmahani, A. Nasiri, M. Malakootian, The application of electrolysis method to disinfect water contaminated by *Salmonella* and *Shigella*, J. Water Chem. Technol., 41 (2019) 182–187.

[17] H. Mahdizadeh, M. Malakootian, Optimization of ciprofloxacin removal from aqueous solutions by a novel semi-fluid Fe/charcoal micro-electrolysis reactor using response surface methodology, Process Saf. Environ. Prot., 123 (2019) 299–308.

[18] M. Malakootian, K. Kannan, M.A. Gharaghani, A. Dehdarirad, A. Nasiri, Y.D. Shahamat, H. Mahdizadeh, Removal of metronidazole from wastewater by Fe/charcoal micro electrolysis fluidized bed reactor, J. Environ. Chem. Eng., 7 (2019) 103457.

[19] J. Liu, Q. Yin, H. Zhang, Y. Yan, Z. Yi, Continuous removal of Cr(VI) and Orange II over a novel Fe0-NaA zeolite membrane catalyst, Sep. Purif. Technol., 209 (2019) 734–740.

[20] M. Malakootian, H. Mahdizadeh, A. Dehdarirad, M. Amiri Gharghani, Photocatalytic ozonation degradation of ciprofloxacin using ZnO nanoparticles immobilized on the surface of stones, J. Dispersion Sci. Technol., 40 (2019) 846–854.

[21] S. Jiménez, M. Andreozzi, M.M. Micó, M.G. Álvarez, S. Contreras, Produced water treatment by advanced oxidation processes, Sci. Total Environ., 666 (2019) 12–21.

[22] G. Moussavi, A. Khavanin, R. Alizadeh, The investigation of catalytic ozonation and integrated catalytic ozonation/biological processes for the removal of phenol from saline wastewaters, J. Hazard. Mater., 171 (2009) 175–181.

[23] M. Malakootian, M. Khatami, H. Mahdizadeh, A. Nasiri, M. Amiri Gharaghani, A study on the photocatalytic degradation of p-Nitroaniline on glass plates by thermo-immobilized ZnO nanoparticle, Inorg. Nano-Metal Chem., 50 (2019) 1–12.

[24] M. Malakootian, A. Nasiri, M. Amiri Gharaghani, Photocatalytic degradation of ciprofloxacin antibiotic by TiO_2 nanoparticles immobilized on a glass plate, Chem. Eng. Commun., 207 (2020) 56–72.

[25] M. Malakootian, A. Nasiri, A. Asadipour, M. Faraji, E. Kargar, A facile and green method for synthesis of $ZnFe_2O_4$@CMC as a new magnetic nanophotocatalyst for ciprofloxacin removal from aqueous media, MethodsX, 6 (2019) 1575–1580.

[26] M. Malakootian, A. Nasiri, A. Asadipour, E. Kargar, Facile and green synthesis of $ZnFe_2O_4$@CMC as a new magnetic nanophotocatalyst for ciprofloxacin degradation from aqueous media, Process Saf. Environ. Prot., 129 (2019) 138–151.

[27] A. Nasiri, F. Tamaddon, M.H. Mosslemin, M. Faraji, A microwave assisted method to synthesize nano$CoFe_2O_4$@methyl cellulose as a novel metal-organic framework for antibiotic degradation, MethodsX, 6 (2019) 1557–1563.

[28] A. Nasiri, F. Tamaddon, M.H. Mosslemin, M.A. Gharaghani, A. Asadipour, New magnetic nanobiocomposite $CoFe_2O_4$@methycellulose: facile synthesis, characterization, and photocatalytic degradation of metronidazole, J. Mater. Sci. - Mater. Electron., 30 (2019) 8595–8610.

[29] M. Malakootian, A. Nasiri, A.N. Alibeigi, H. Mahdizadeh, M.A. Gharaghani, Synthesis and stabilization of ZnO nanoparticles on a glass plate to study the removal efficiency of Acid Red 18 by hybrid advanced oxidation process (ultraviolet/ZnO/ultrasonic), Desal. Wat. Treat., 170 (2019) 325–336.

[30] A.K. Arora, V.S. Jaswal, K. Singh, R. Singh, Applications of metal/mixed metal oxides as photocatalyst: a review, Orient. J. Chem., 32 (2016) 2035–2042.

[31] N. Sobana, M. Swaminathan, The effect of operational parameters on the photocatalytic degradation of Acid Red 18 by ZnO, Sep. Purif. Technol., 56 (2007) 101–107.

[32] D. Rajamanickam, M. Shanthi, Photocatalytic degradation of an organic pollutant by zinc oxide–solar process, Arabian J. Chem., 9 (2016) S1858–S1868.

[33] S. Saeid, P. Tolvanen, N. Kumar, K. Eränen, J. Peltonen, M. Peurla, J.-P. Mikkola, A. Franz, T. Salmi, Advanced oxidation process for the removal of ibuprofen from aqueous solution: a non-catalytic and catalytic ozonation study in a semi-batch reactor, Appl. Catal., B, 230 (2018) 77–90.

[34] E. Rahimi, Y.D. Shahamat, B. Kamarehei, A. Zafarzadeh, M. Khani, Rapid decolorization and mineralization of molasses by catalytic ozonation process with a nanocomposite from fermentation industry wastewater, Int. J. Environ. Sci. Technol., 15 (2018) 1941–1948.

[35] N. Daneshvar, D. Salari, A. Khataee, Photocatalytic degradation of azo dye acid red 14 in water on ZnO as an alternative catalyst to TiO_2, J. Photochem. Photobiol., A, 162 (2004) 317–322.

[36] A. Ikhlaq, D.R. Brown, B. Kasprzyk-Hordern, Catalytic ozonation for the removal of organic contaminants in water on alumina, Appl. Catal., B, 165 (2015) 408–418.

[37] D.R. Vakilabadi, A.H. Hassani, G. Omrani, B. Ramavandi, Catalytic potential of Cu/Mg/Al-chitosan for ozonation of real landfill leachate, Process Saf. Environ. Prot., 107 (2017) 227–237.

[38] E. Darezereshki, M. Alizadeh, F. Bakhtiari, M. Schaffie, M. Ranjbar, A novel thermal decomposition method for the synthesis of ZnO nanoparticles from low concentration $ZnSO_4$ solutions, Appl. Clay Sci., 54 (2011) 107–111.

[39] M.I. Khalil, M.M. Al-Qunaibit, A.M. Al-Zahem, J.P. Labis, Synthesis and characterization of ZnO nanoparticles by thermal decomposition of a curcumin zinc complex, Arabian J. Chem., 7 (2014) 1178–1184.

[40] J. Yu, X. Yu, Hydrothermal synthesis and photocatalytic activity of zinc oxide hollow spheres, Environ. Sci. Technol., 42 (2008) 4902–4907.

[41] S. Kundu, A. Pal, A.K. Dikshit, UV induced degradation of herbicide 2, 4-D: kinetics, mechanism and effect of various conditions on the degradation, Sep. Purif. Technol., 44 (2005) 121–129.

[42] J. Staehelin, R. Buehler, J. Hoigné, Ozone decomposition in water studied by pulse radiolysis. 2. Hydroxyl and hydrogen tetroxide (HO_4) as chain intermediates, J. Phys. Chem., 88 (1984) 5999–6004.

[43] T.A. Kurniawan, W.-h. Lo, G. Chan, Radicals-catalyzed oxidation reactions for degradation of recalcitrant compounds from landfill leachate, Chem. Eng. J., 125 (2006) 35–57.

[44] A. Ikhlaq, D.R. Brown, B. Kasprzyk-Hordern, Catalytic ozonation for the removal of organic contaminants in water on ZSM-5 zeolites, Appl. Catal., B, 154–155 (2014) 110–122.

[45] A. Hassani, A. Khataee, M. Fathinia, S. Karaca, Photocatalytic ozonation of ciprofloxacin from aqueous solution using TiO_2/MMT nanocomposite: nonlinear modeling and optimization of the process via artificial neural network integrated genetic algorithm, Process Saf. Environ. Prot., 116 (2018) 365–376.

[46] N.M. Mahmoodi, Photocatalytic ozonation of dyes using copper ferrite nanoparticle prepared by co-precipitation method, Desalination, 279 (2011) 332–337.

[47] Z. Bai, Q. Yang, J. Wang, Catalytic ozonation of sulfamethazine using $Ce_{0.1}Fe_{0.9}OOH$ as catalyst: mineralization and catalytic mechanisms, Chem. Eng. J., 300 (2016) 169–176.

[48] V. Vaiano, M. Matarangolo, J. Murcia, H. Rojas, J. Navío, M. Hidalgo, Enhanced photocatalytic removal of phenol from aqueous solutions using ZnO modified with Ag, Appl. Catal., B, 225 (2018) 197–206.

[49] A. Khataee, M. Kıranşan, S. Karaca, M. Sheydaei, Photocatalytic ozonation of metronidazole by synthesized zinc oxide nanoparticles immobilized on montmorillonite, J. Taiwan Inst. Chem. Eng., 74 (2017) 196–204.

[50] S. Pirgalıoğlu, T.A. Özbelge, Comparison of non-catalytic and catalytic ozonation processes of three different aqueous single dye solutions with respect to powder copper sulfide catalyst, Appl. Catal., A, 363 (2009) 157–163.

[51] B. Kasprzyk-Hordern, M. Ziółek, J. Nawrocki, Catalytic ozonation and methods of enhancing molecular ozone reactions in water treatment, Appl. Catal., B, 46 (2003) 639–669.

[52] J.B. Parsa, M. Golmirzaei, M. Abbasi, Degradation of azo dye C.I. Acid Red 18 in aqueous solution by ozone-electrolysis process, J. Ind. Eng. Chem., 20 (2014) 689–694.

[53] R. Parvarideh, S. Karimzadeh, H. Khorsandi, S. Jafari, A. Aghapour, A comparison of single and catalytic ozonation for decolorization of malachite green, Desal. Wat. Treat, 152 (2019) 411–418.

[54] A. Zuorro, R. Lavecchia, Evaluation of UV/H_2O_2 advanced oxidation process (AOP) for the degradation of diazo dye Reactive Green 19 in aqueous solution, Desal. Wat. Treat, 52 (2014) 1571–1577.

[55] C. Orge, J. Faria, M. Pereira, Photocatalytic ozonation of aniline with TiO_2-carbon composite materials, J. Environ. Manage., 195 (2017) 208–215.